ELSEVIER

International Journal of Mass Spectrometry 201 (2000) 161–177

International Journal of Mass Spectrometry

Intramolecular hydrogen migrations in ionized aliphatic alcohols. Barton type and related rearrangements

Guy Bouchoux*, Nadège Choret

Département de Chimie, Laboratoire des Mécanismes Réactionnels, UMR CNRS 7651, Ecole Polytechnique, 91128 Palaiseau cedex, France

Received 4 October 1999; accepted 29 November 1999

Abstract

Molecular orbital calculations at the unified G2(MP2, SVP) level of theory have been used to examine the energy barrier for 1,*n*-hydrogen atom migrations in ionized aliphatic alcohols $[H(CH_2)_{n-1}OH]^{\cdot+} \rightarrow [(CH_2)_{n-1}OH_2]^{\cdot+}$ (n = 2–5). A complementary set of experimental and theoretical data confirm that this approach leads to results accurate to within a few kJ mol^{-1}. The better stability of distonic ions $[(CH_2)_{n-1}OH_2]^{\cdot+}$ with respect to their classical homologs $[H(CH_2)_{n-1}OH]^{\cdot+}$ is clearly demonstrated by the calculations; it amounts to ~30 kJ mol^{-1}. Critical energies of 106, 90, 76, and 19 kJ mol^{-1} are calculated for n = 2, 3, 4, and 5, respectively. A lowering of the barrier height is observed when considering the energy barrier for 1,5 hydrogen atom migrations in ionized systems with respect to the neutral equivalent, i.e. the Barton rearrangement. (Int J Mass Spectrom 201 (2000) 161–177) © 2000 Elsevier Science B.V.

Keywords: Ionized alcohols; Hydrogen migrations; Distonic ions; α2(MP2,SVP) molecular orbital calculations.

1. Introduction

Intramolecular H atom migrations play an important role in the chemistry of open-shell molecular systems. Their participation in the reactivity of carbon or heteroatom centered radicals [1] as well as that of ionized species [2] is well established. Knowledge of the corresponding activation energies is crucial to the understanding of this particular chemistry. However, in some instances the experimental determination of such quantities can be rather difficult and theoretical calculations may offer a suitable alternative.

The activation energy of the 1,*n*-hydrogen atom migrations depends on the nature of the two atoms supporting the H atom transfer and on the number (n) of atoms in the chain including these atoms. The generally accepted values for the activation energy of 1,*n*-H migration on carbon centered radicals is 20–40 kJ mol^{-1} for 1,5-H; 60–90 kJ mol^{-1} for 1,4-H; and ~150 kJ mol^{-1} for 1,3 or 1,2-H transfers [1,3]. Similarly, an activation energy close to 40 kJ mol^{-1} has been determined, both experimentally [1] and theoretically [4], for the Barton type rearrangement [5]. In the case of radical cations, a molecular orbital study has been devoted to 1,*n*-H migration in ionized amines [6]. The predicted critical energies were ~20, 70, 140, and 170 kJ mol^{-1} for 1,5-, 1,4-, 1,3-, and 1,2-H migrations, respectively. Comparable results

* Corresponding author. E-mail: bouchoux@dcmr.polytechnique.fr

PII S1387-3806(00)00158-5

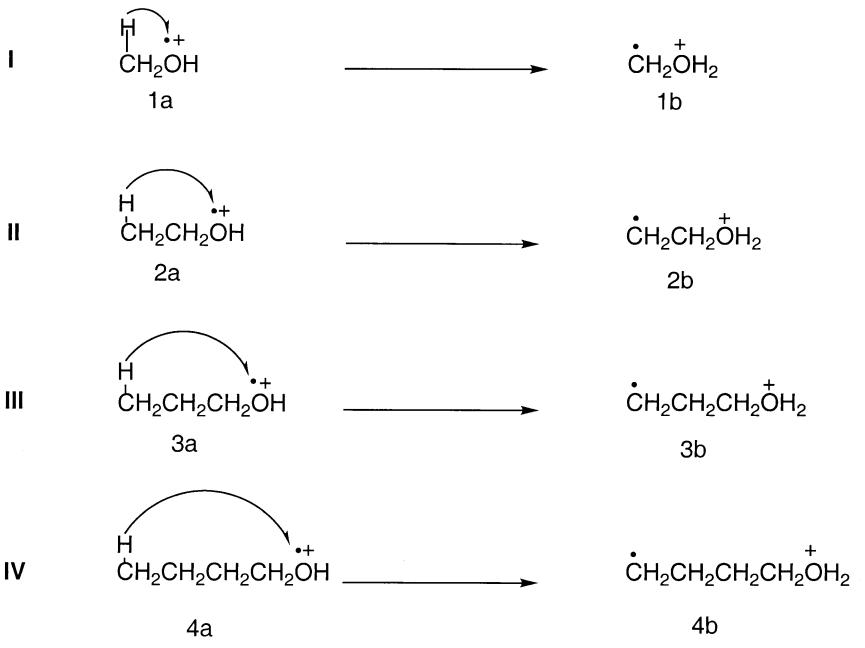

Scheme 1.

were obtained for internal H atom transfers to the oxygen of carbonyl radical cations [2,7] (critical energies of ≈15, 65, 115, and 210 kJ mol^{-1} are associated with 1,5- [7a,b], 1,4- [7c], 1,3- [7c], and 1,2-H [7d] migrations, respectively). To date, only fragmentary data is available for ionized alcohols $[H(CH_2)_{n-1}OH]^{\cdot +}$ [8,9]. In particular, no systematic study has been devoted to reactions leading to distonic ions $[(CH_2)_{n-1}OH_2]^{\cdot +}$ even though the major dissociation process of ionized alcohols, the water loss, probably involves the intermediacy of such species [10]. The present study reports the results of ab initio molecular orbital calculations conducted at the unified G2(MP2, SVP) level of theory on the prototypical reactions I–IV (Scheme 1).

2. Computational section

Standard ab initio calculations have been carried out using the GAUSSIAN 94 series of programs [11]. Initially, the geometries of the different species investigated were optimized at the HF/6-31G* level; the zero point energy (ZPE) of the species considered has been calculated at this level after scaling by a factor 0.8929 [12]. The HF/6-31G* geometries were then refined at the MP2(FrozenCore)/6-31G* level to take electron correlation effects explicitly into account. The corresponding harmonic vibrational frequencies were again calculated in order to verify that the stationary points found were local minima or transition structures on the potential energy surface.

It has been established that accurate heats of formation of open-shell systems can be obtained from calculations at the G2 level of theory or its variants, G2(MP2) and G2(MP2, SVP), for species with low spin contamination [13]. For the open-shell species investigated here, the unprojected ⟨S2⟩ values were within 0.758−0.782, indicating negligible spin contamination. Standard G2 theory [14] employs a geometry optimized at the MP2(full)/6-31G(d) level and a scaled HF/6-31G(d) ZPE. A base energy calculated at the MP4/6-311G(d,p) level is corrected by several additivity approximations to QCISD(T) and to the 6-311+G(3df,2p) basis set. In an attempt to account for residual basis set deficiencies, G2 theory introduces higher-level corrections (HLC) that depend on

the number of paired and unpaired electrons. Unfortunately, for the systems of the size investigated here, the MP4 calculations are particularly expensive and, consequently, the use of a cheaper alternative such as G2(MP2) [15] or G2(MP2, SVP) [16] is required. In the G2(MP2) variant, the basis set extension corrections are evaluated at the MP2 level, whereas energies are calculated at the QCISD(T)/6-311G(d,p) level. The total energy E[G2(MP2)] is given by Eq. (1):

$$\begin{aligned} \mathrm{E[G2(MP2)]} = {} & \mathrm{E[QCISD(T)/6\text{-}311G(d,p)]} \\ & + \mathrm{E[MP2/6\text{-}311{+}G(3df,2p)]} \\ & - \mathrm{E[MP2/6\text{-}311G(d,p)]} \\ & + \mathrm{HLC} + \mathrm{ZPE} \end{aligned} \quad (1)$$

In the G2(MP2, SVP) procedure the QCISD(T) calculations are carried out using the split-valence plus polarization (SVP) 6-31G(d) basis set. At this level, E[G2(MP2, SVP)] is given by Eq. (2):

$$\begin{aligned} \mathrm{E[G2(MP2,\,SVP)]} = {} & \mathrm{E[QCISD(T)/6\text{-}31G(d)]} \\ & + \mathrm{E[MP2/6\text{-}311{+}G(3df,2p)]} \\ & - \mathrm{E[MP2/6\text{-}31G(d)]} \\ & + \mathrm{HLC} + \mathrm{ZPE} \end{aligned} \quad (2)$$

In both cases the HLC correction is calculated from Eq. (3):

$$\mathrm{HLC} = -A\, n_\beta - B\, n_\alpha \quad (3)$$

with n_β and n_α being the number of β and α valence electrons, respectively ($n_\beta < n_\alpha$), and the parameters A and B equal to 5.13 10^{-3} and 0.19 10^{-3} Hartree, respectively [16].

In the present study, optimized geometries were obtained using the frozen core approximation at the MP2/6-31G* level (i.e. MP2(fc)/6-31G*). Restricted (RHF, RMP2) and unrestricted (UHF, UMP2) procedures were used for closed- and open-shell systems, respectively.

Heats of formation of the species involved in reactions I–IV have been evaluated from G2(MP2, SVP) total energies by two means. The first procedure uses calculated atomization energies; the second employs calculated dissociation energies.

In the first method, heats of formation at 0 K ($\Delta_f H_0^\circ$) were obtained from the calculated G2(MP2, SVP) total energies via atomization reactions [16b]. Thus, for a given species X, $\Delta_f H_0^\circ(X)$ is given by Eq. (4):

$$\begin{aligned} \Delta_f H_0^\circ(X) = {} & \Sigma \Delta_f H_0^\circ(\mathrm{atoms}) \\ & - \Sigma \mathrm{E[G2(MP2,\,SVP)](atoms)} \\ & + \mathrm{E[G2(MP2,\,SVP)]}(X) \end{aligned} \quad (4)$$

The heat of formation at 298 K is therefore given by Eq. (5):

$$\begin{aligned} \Delta_f H_{298}^\circ(X) = {} & \Delta_f H_0^\circ(X) + \Delta_{298} H^\circ(X) \\ & - \Sigma \Delta_{298} H^\circ(\mathrm{elements}) \end{aligned} \quad (5)$$

where the difference between the enthalpy at 298 K and 0 K is represented by the terms $\Delta_{298}H^\circ$ ($\Delta_{298}H^\circ = H_{298}^\circ - H_0^\circ$). For the elements, experimental $\Delta_{298}H^\circ$ values have been used (i.e. 8.468, 1.050, and 8.68 kJ mol^{-1} for $H_{2(g)}$, $C_{(s)}$, and $O_{2(g)}$, respectively), whereas, for the other species, the translational and rotational contributions were taken equal to 3 RT and the vibrational contribution estimated from the scaled (by a factor 0.8929) HF/6-31G* vibrational frequencies.

The second means to obtain $\Delta_f H_{298}^\circ(X)$ is to combine the 298 K calculated enthalpy variation of a given reaction $X \rightarrow Y$ and the known heat of formation of Y. This procedure has been applied to various dissociation reactions of species X = **1a**–**4a** for which accurate heats of formation of the reactants (Y) were available [17].

All the calculated 298 K standard heats of formation presented in Tables 1, 3, 5, and 7 refer to a mean value of the G2(MP2, SVP) results averaged over the two methods indicated above; the associated standard deviation is also indicated.

The optimized MP2(fc)/6-31G* geometries of the different systems included in this study are presented in Fig. 1. The corresponding total and relative energies estimated at various levels of theory are discussed in the text.

3. Results and discussion

3.1. $[CH_3OH]^{\cdot+}/[CH_2OH_2]^{\cdot+}$

Since 1982, this system has been thoroughly studied both experimentally [18,19] and theoretically [8,20,21]. We thus concentrate here on the relevance

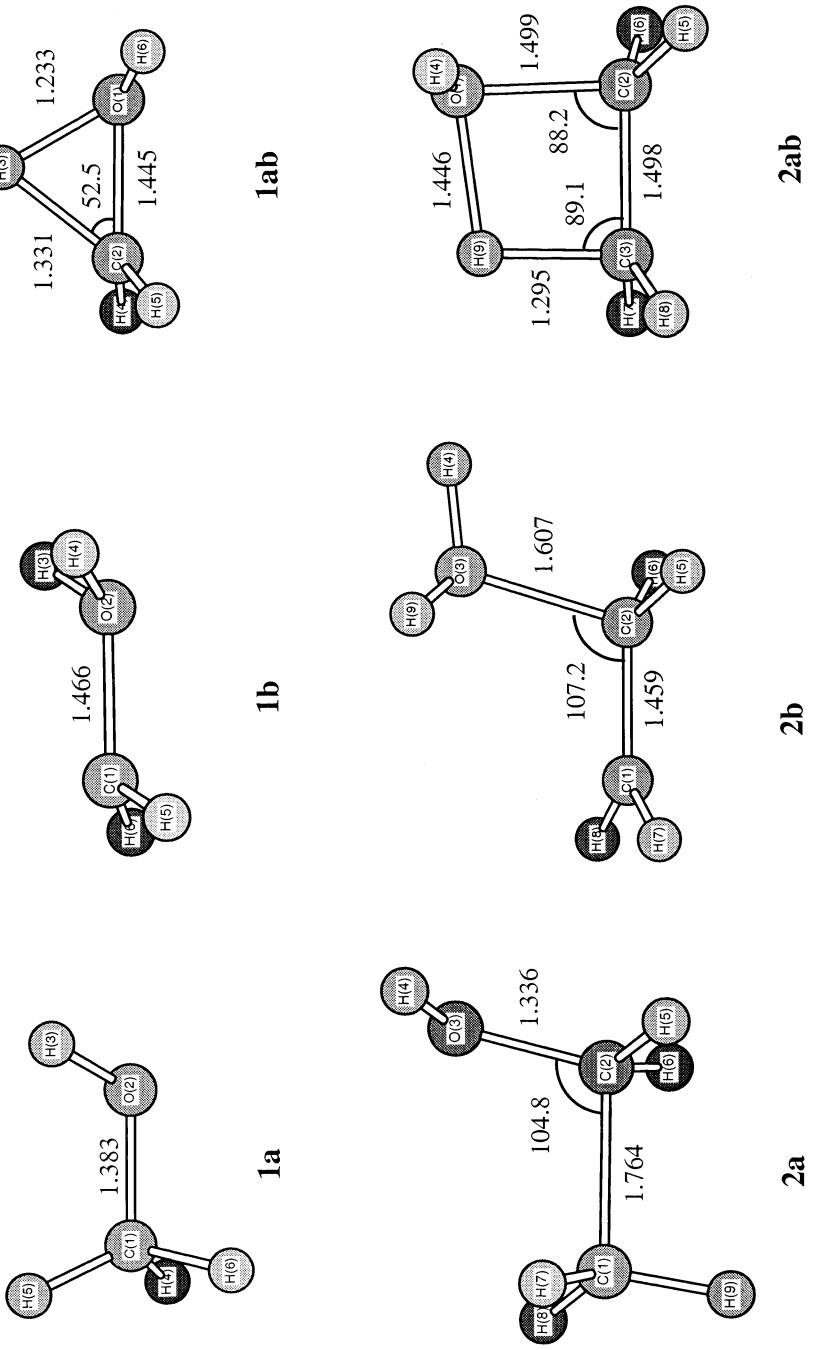

Fig. 1. Selected geometrical parameters (angles in degrees, lengths in Å) of the MP2(fc)/6-31G* optimized geometries of the ions considered.

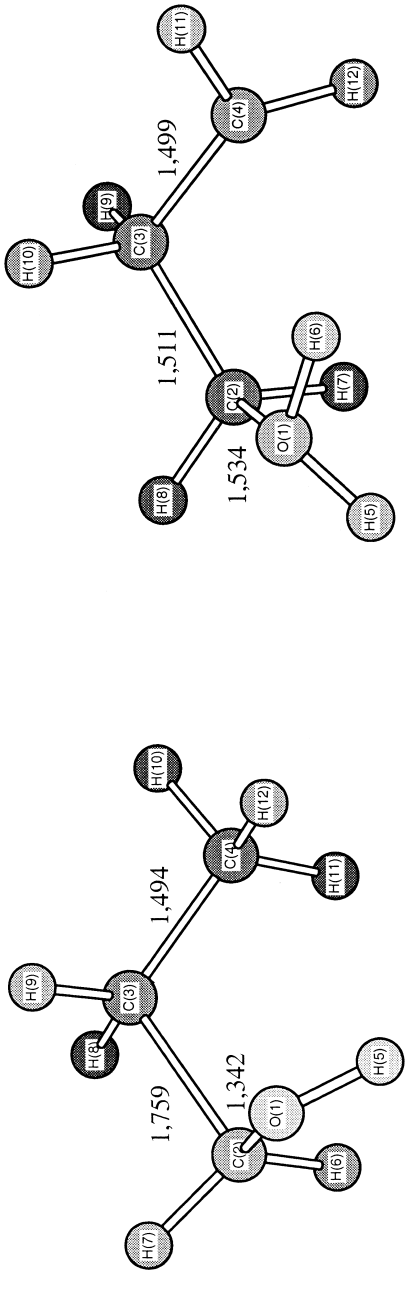

3a

3b

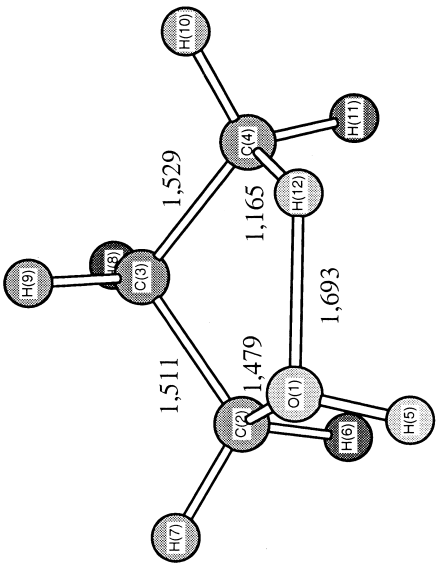

3ab

Fig. 1. *(continued)*

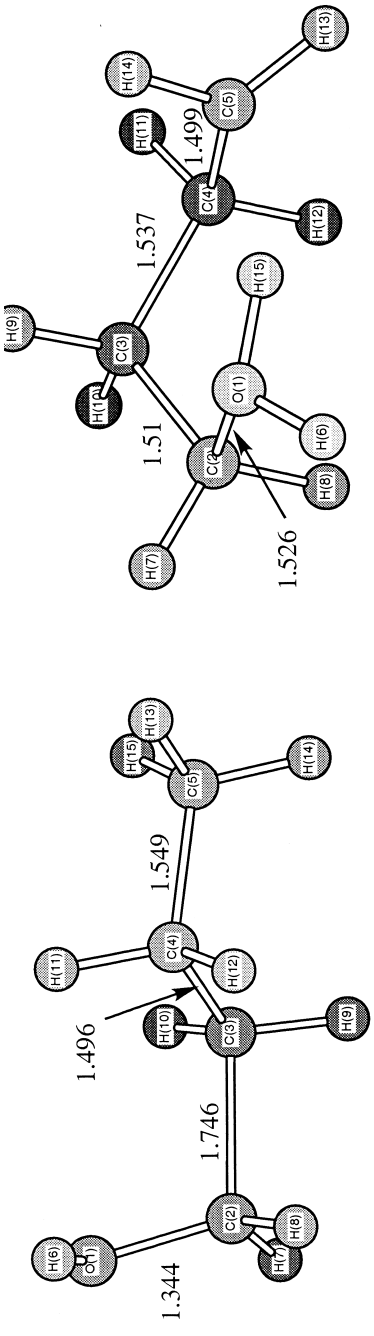

4a

4b

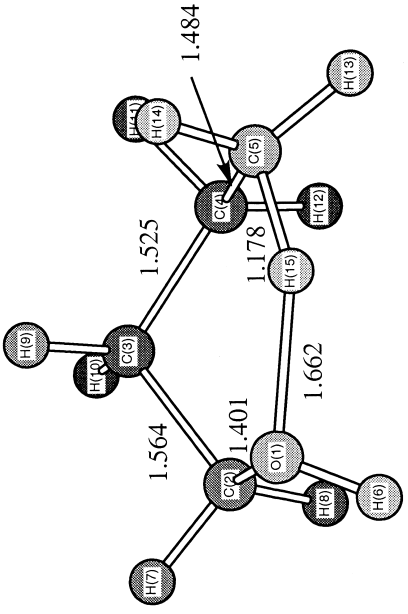

4ab

Fig. 1. *(continued)*

Table 1
Experimental and calculated heats of formation (kJ mol^{-1}) relevant to the $[CH_3OH]^{\cdot+}/[CH_2OH_2^+]$ system

Species	$\Delta_f H^\circ_{298}$(exp)[a]	$\Delta_f H^\circ_{298}$(calc)[b]
$CH_3OH^{\cdot+}$, **1a**	845 ± 2	856 ± 4
$^{\cdot}CH_2OH_2^+$, **1b**	818 ± 9	824 ± 4
Transition structure, **1ab**	>926	960 ± 4
CH_2OH^+	708	
$H^{\cdot}$	218	
$CH_2OH^+ + H^{\cdot}$, **1c**	926	

[a] From [17] unless otherwise specified.
[b] Mean G2(MP2, SVP) value estimated from the atomization energies and heat of reactions leading to **1c**.

of the G2(MP2, SVP) procedure to correctly describe the energetics of the isomerization process **1a** → **1b**. The experimental heat of formation of ionized methanol, $\Delta_f H^\circ$(**1a**) = 845 ± 2 kJ mol^{-1}, can be determined from $\Delta_f H^\circ$(methanol) = −202 kJ mol^{-1} [17] and the adiabatic ionization energy, IE(methanol) = 10.84 eV [18,19]. Concerning the distonic ion $[CH_2OH_2]^{\cdot+}$, **1b**, a heat of formation of $\Delta_f H^\circ$(**1b**) = 818 ± 9 kJ mol^{-1} is obtained by using the experimental proton affinity of $^{\cdot}CH_2OH$ (695 ± 8 kJ mol^{-1} [22]) and the most recently determined heat of formation value of this radical (−17 ± 1 kJ mol^{-1} [23]) (Table 1).

Several experimental arguments indicate that $[CH_3OH]^{\cdot+}$, **1a**, and $[CH_2OH_2]^{\cdot+}$, **1b**, are distinct species that do not interconvert easily. Both ions **1a** and **1b** of low internal energy eliminate a hydrogen atom, but with distinct characteristics. Accordingly, the values of the translational energy released during the separation of the fragments are different. These terms, estimated from the metastable peak width at half height, are 9 ± 2 meV for **1a** and 34 ± 2 meV from **1b** [18c]. On the other hand, the collision induced dissociation spectrum of **1a** is dominated by $OH^{\cdot}$ loss whereas that of **1b** exhibits an intense signal at *m/z* 14 due to water loss. Furthermore, deuterium labeling indicates that no interconversion occurs between isomers **1a** or **1b** sampled during collisional experiments. Thus the stable ions **1a** and **1b** keep their structural identity up to the dissociation threshold leading to $[CH_2OH]^+ + H^{\cdot}$, i.e. 81 kJ mol^{-1} above **1a** (Table 1).

Extensive ab initio molecular orbital calculations have been carried out on this system at various levels of theory. The present G2, G2(MP2), and G2(MP2, SVP) results are reported in Table 2 together with some of the most recently published data [8b,8c,20]. For the purpose of comparison the G2(MP2, SVP) computed heats of formations, estimated from atomization energies and enthalpies of the dissociation

Table 2
Calculated total (hartree) and relative (kJ mol^{-1}) energies involving the $[CH_3OH]^{\cdot+}/[CH_2OH_2^+]$ system

Level of theory	E(**1a**)	ΔE(**1b**)[a]	ΔE(**1ab**)[a]	ΔE(**1c**)[a] ($CH_2OH^+ + H^{\cdot}$)
HF/6-31G*	−114.68722	−15	182	
ZPE (HF/6-31G*)	122	124	113	103
MP2/6-31G*	−114.954579	−49	102	
QCISD(T)/6-31G*	−114.99571	−19	127	49
MP2/6-311G(d,p)	−115.03783	−61	89	
QCISD(T)/6-311G(d,p)	−115.08146	−32	112	
MP2/6-311+G(3df,2p)	−115.10126	−62	80	27
G2(MP2)	−115.12879	−33 (−34)	104 (102)	
G2(MP2, SVP)	−115.12821	−31 (−32)	106 (104)	63 (66)
G2	−115.13220	−32 (−32)	105 (103)	
G2′[b]		−27 (−27)		
G2**[c]		−29 (−29)	108 (108)	

[a] Relative energies including ZPE corrections or, in parentheses, 298 K enthalpy corrections.
[b] Based on MP2/6-311+G** optimized geometries [20].
[c] Based on MP2/6-31G** optimized geometries [8c]; similar results are obtained at the QCISD/6-31G** level [8b].

reactions leading to $[CH_2OH]^+ + H^{\cdot}$, are quoted beside their experimental counterparts in Table 1.

From examination of the five last lines of Table 2, it is clear that the computed relative energy of species **1a**, **1b**, and **1ab**, is independent of the level of refinement used in the G2 theory. For example, the 298 K G2(MP2, SVP) enthalpies of **1b** and **1ab**, with respect to **1a**, are −32 and 104 kJ mol^{-1}, respectively, whereas the values given by the more sophisticated G2** method are −29 and +108 kJ mol^{-1}, respectively. This comparison leads to the expectation that the G2(MP2, SVP) level of calculations will provide a correct picture of the energetics of the reactions under study. Another way to test the accuracy of the theory is to compare its results with the relevant experimental data, from which it is evident that the experimental relative enthalpy of isomers **1a** and **1b** (−27 ± 11 kJ mol^{-1}) is correctly reproduced by the calculations [−31 kJ mol^{-1}, G2(MP2, SVP) results]. Moreover, theoretical estimates of $\Delta_f H^\circ_{298}$ for **1a** and **1b** using G2(MP2, SVP) atomization or dissociation energies, are in correct agreement with their experimentally derived heats of formation (Table 1).

In summary, G2(MP2, SVP) theory appears to be the method of choice for the present investigation, because both the relative enthalpy of structures **1a**, **1b**, and **1c** and the critical energy associated with the isomerization **1a** → **1b** are satisfactorily estimated. The present results confirm that the 1,2-hydrogen atom migration, **1a** → **1b** (reaction I), requires an activation energy only slightly above 100 kJ mol^{-1}. This is in agreement with experiment which indicates a lower limit of 81 kJ mol^{-1} for this energy barrier.

3.2. $[C_2H_5OH]^{\cdot+}/[C_2H_4OH_2]^{\cdot+}$

The adiabatic ionization energy of ethanol IE(ethanol) = 10.47 eV [19] combined with $\Delta_f H°$(ethanol) = −235 kJ mol^{-1} [17] leads to $\Delta_f H°$(**2a**) = 775 ± 2 kJ mol^{-1} (Table 3). From the appearance energy measurement of the $[C_2H_6O]^{\cdot+}$ fragment ion originating from electron ionization of 2-methoxyethanol [18c], a heat of formation of 732 ± 5 kJ mol^{-1} has been deduced for the distonic ion $[C_2H_4OH_2]^{\cdot+}$, **2b**. Another estimate of the heat of formation of distonic ions such as **2b** may be derived from a simple thermodynamic cycle [8f]. As depicted in Scheme 2, ion **2b** may be seen as the result of hydrogen atom abstraction from protonated ethanol **2H$^+$** or as the oxygen protonated form of the free radical $^{\cdot}CH_2CH_2OH$, [**2-H**].

The $\Delta_f H^\circ_{298}$ of the distonic ion $^{\cdot}CH_2CH_2OH_2^+$ may thus be calculated using the relationships Eq. (6):

Table 3
Experimental and calculated heats of formation (kJ mol^{-1}) relevant to the $[CH_3CH_2OH]^{\cdot+}/[CH_2CH_2OH_2^+]$ system

Species	$\Delta_f H^\circ_{298}$(exp)[a]	$\Delta_f H^\circ_{298}$(calc)[b]
$CH_3CH_2OH^{\cdot+}$, **2a**	775 ± 2	772 ± 4
$^{\cdot}CH_2CH_2OH_2^+$, **2b**	732 ± 5 (731)[c]	735 ± 4
Transition structure, **2ab**	824 < **2ab** < 923	859 ± 4
CH_3CHOH^+	595	
$H^{\cdot}$	218	
$CH_3CHOH^+ + H^{\cdot}$, **2c**	813	
$CH_2{=}CH_2^{\cdot+}$	1066	
H_2O	−242	
$CH_2{=}CH_2^{\cdot+} + H_2O$, **2d**	824	
$^+CH_2OH$	708	
$^{\cdot}CH_3$	146	
$^+CH_2OH + {}^{\cdot}CH_3$, **2e**	854	

[a] [17] unless otherwise specified.
[b] Mean value estimated from the G2(MP2, SVP) atomization and dissociation energies.
[c] Value estimated from the thermodynamic cycle depicted in the text, using the relationship (6c) with $\Delta_f H°(C_2H_5OH)$ = −235 kJ mol^{-1}; IE($H^{\cdot}$) = 1312 kJ mol^{-1}; BDE(RCH_2-H) = 430 kJ mol^{-1} and PA(C_2H_5OH) = 776 kJ mol^{-1} (all data are taken from [17]).

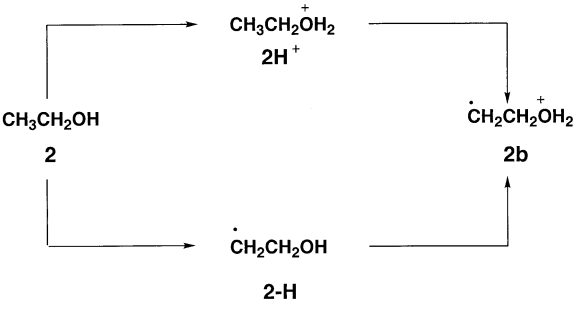

Scheme 2.

$$\Delta_f H^\circ[\mathbf{2b}] = \Delta_f H^\circ(\mathbf{2}) - \mathrm{PA}(\mathbf{2}) + \mathrm{BDE}(\mathbf{2H^+}) + \mathrm{IE}(H^\cdot) \quad (6a)$$

$$\Delta_f H^\circ[\mathbf{2b}] = \Delta_f H^\circ(\mathbf{2}) + \mathrm{BDE}(\mathbf{2}) - \mathrm{PA}(\mathbf{2\text{-}H}) + \mathrm{IE}(H^\cdot) \quad (6b)$$

where BDE means bond dissociation energy; PA, proton affinity; and IE, ionization energy. In general, BDE(**2H$^+$**) and PA(**2-H**) are poorly documented values. The usual approximation consists of considering that BDE(**2H$^+$**) ≈ BDE(**2**) or that PA(**2-H**) ≈ PA(**2**) and consequently to write:

$$\Delta_f H^\circ[\mathbf{2b}] \approx \Delta_f H^\circ(\mathbf{2}) + \mathrm{BDE}(\mathbf{2}) - \mathrm{PA}(\mathbf{2}) + \mathrm{IE}(H^\cdot) \quad (6c)$$

A value of $\Delta_f H^\circ[\mathbf{2b}] = 731$ kJ mol^{-1} is obtained when using this approximation and the relevant data reported in Table 3.

The two structures **2a** and **2b** can be readily characterized by their spontaneous unimolecular or collision induced dissociations. For example, metastable ion **2a** loses a hydrogen atom whereas **2b** exclusively eliminates a water molecule [24]. The thermochemical thresholds for both reactions are 38 and 49 kJ mol^{-1}, respectively, with respect to the energy level of ionized ethanol (Table 3). Deuterium labeled ions $[C_2H_4OD_2]^{\cdot+}$ specifically eliminate D_2O, demonstrating that no hydrogen exchange between the oxygen and the two carbon atoms occurs before dissociation. From this result, and from the lack of elimination of H from **2b**, one may conclude that the critical energy for isomerization **2a** → **2b** is greater than 49 kJ mol^{-1}. Collisional experiments (low energy collisional activation [25], high energy collisional activation, and neutralisation–reionization [26]) also demonstrate clearly that the two ions **2a** and **2b** are structurally distinct and thus separated by an energy barrier higher than the energy of the products $[C_2H_4]^{\cdot+} + OH_2$. The appearance energy of $[C_2H_4]^{\cdot+}$ ions from **2a** has been determined by photoionization [19]. This determination, which includes a large kinetic shift because dehydration is not the process of lowest energy from **2a**, gives only an upper limit (of 148 kJ mol^{-1}) for the critical energy of the isomerization **2a** → **2b**.

The MP2/6-31G* optimized geometries generally compare well with those calculated by Radom and co-workers, at a higher level of theory [27]. In the case of ionized ethanol, **2a**, a particularly long C–C bond (1.764 Å) is predicted at the MP2/6-31G* level (Fig. 1). In this most stable conformation, the hydroxylic hydrogen is perpendicular to the C–C bond. Note that the CC bond elongation is accompanied by a shortening of the C–O bond (1.336 Å, compared to 1.383 Å in ionized methanol **1a**). Thus the structure resembles the dissociation products $[CH_2OH]^+ + {}^\cdot CH_3$. This is corroborated by the fact that the spin density at the terminal carbon is almost equal to 0.5. For **2b**, the C–O bond length is equal to 1.607 Å (Fig. 1), i.e. longer than in the distonic ion **1b** (1.465 Å); again this structural feature is reminiscent of the energetically favoured dissociation products $[C_2H_4]^{\cdot+} + OH_2$. The transition structure **2ab** is characterized by C . . . H and O . . . H bonds of 1.295 and 1.446 Å, respectively. In agreement with Hammond's postulate, these values are close to those of the species closest in energy, i.e. the reactant **2a**.

A summary of the energies calculated for **2a**, **2b**, and **2ab** is given in Table 4. In order to confirm the validity of the G2(MP2, SVP) calculations, the energy levels of three possible sets of dissociation products were also considered. These species are: $[CH_3CHOH]^+ + H^\cdot$, **2c**, $[CH_2{=}CH_2]^{\cdot+} + H_2O$, **2d**, and $[CH_2OH]^+ + {}^{52}CH_3$, **2e**. As recalled above, the first two pairs are the low energy dissociation products of ions **2a** and **2b**, respectively. Obviously, fragments **2e** are also possible dissociation products of ions **2a**. The calculated G2(MP2, SVP) relative 298 K enthalpy levels of these various reaction products are also reported in Table 4. A comparison between Tables 3 and 4 shows that the experimental 298 K enthalpy differences between **2c–2e** and **2a** are reproduced within 4 kJ mol^{-1} by the G2(MP2, SVP) calculations. It appears also, from examination of Table 4, that a remarkably good agreement between the G2, G2(MP2), and G2(MP2, SVP) values for the 298 K enthalpy difference between **2a** and **2b** is obtained. This value, −37 kJ mol^{-1}, is also very close

Table 4
Calculated total (hartree) and relative (kJ mol^{-1}) energies involving the $[CH_3CH_2OH]^{\cdot+}/[CH_2CH_2OH_2^+]$ system

Level of theory	E(**2a**)	ΔE(**2b**)[a]	ΔE(**2ab**)[a]	ΔE(**2c**)[a] ($CH_3CHOH^+ + H^{\cdot}$)	ΔE(**2d**)[a] ($C_2H_4^+ + H_2O$)	ΔE(**2e**)[a] ($CH_2OH^+ + CH_3^{\cdot}$)
HF/6-31G*	−153.73685	−48	143			
ZPE(HF/6-31G*)	194	194	187	173	166	175
MP2(FC)/6-31G*	−154.15121	−36	102	0	68	80
QCISD(T)/6-31G*	−154.19853	−35	92	11	67	74
MP2/6-311G(d,p)	−154.26357	−42	101			
QCISD(T)/6-311G(d,p)	−154.31645	−40	93			
MP2/6-311+G(3df,2p)	−154.35381	−39	99	22	47	81
G2(MP2)	−154.37797	−37 (−36)	91 (88)			
G2(MP2, SVP)	−154.37529	−38 (−37)	90 (87)	33 (37)	45 (53)	76 (82)
G2	−154.38188	−37 (−36)				

[a] Relative energies including ZPE corrections or, in parentheses, 298 K enthalpy corrections.

to the experimental difference in heats of formation of these two species (−43 ± 7 kJ mol^{-1}, Table 3). Calculation of the heat of formation of the two isomers using the G2(MP2, SVP) atomization or dissociation energies is also in excellent agreement with experiment (see Table 3).

The last important information provided by the calculation is the height of the barrier for 1,3-H migration **2a** → **2b** (reaction II). Again, G2(MP2) and G2(MP2, SVP) methods give identical results (Table 4) suggesting that the value of 88 kJ mol^{-1} may be confidently considered the critical energy of this reaction. As expected from the experimental observations, the enthalpy level of the transition structure **2ab** (calculated value = 860 kJ mol^{-1}) is higher than that of the dissociation products $[C_2H_4]^{\cdot+}$ + OH_2 (824 kJ mol^{-1}) and lower than the upper limit given by the photoionization experiments (923 kJ mol^{-1}) (Table 3).

3.3. $[C_3H_7OH]^{\cdot+}/[C_3H_6OH_2]^{\cdot+}$

The thermochemistry of ionized propanol **3a** has been investigated by photoionization experiments [19,28,29b]. The photoionization onset of 10.22 eV, attributed to the adiabatic ionization energy, combined with $\Delta_fH°$(propanol) = −255 kJ mol^{-1}, leads to $\Delta_fH°$(**3a**) = 731 kJ mol^{-1} (Table 5). In 1984, Holmes et al. [30] demonstrated that the distonic ion $[CH_2CH_2CH_2OH_2]^{\cdot+}$, **3b**, may be formed by CH_2O loss from ionized 1,4-butane diol. From the determination of the appearance energy of the fragment ion **3b** they deduced a heat of formation, $\Delta_fH°$(**3b**), of 714 ± 5 kJ mol^{-1}. Another estimate of the latter may be obtained from a thermochemical cycle by the procedure that has proven to be correct in predicting the heat of formation of **2b** [Scheme 2 and Eq. (6)]. In this approach, the $\Delta_fH°$ of the distonic ion

Table 5
Experimental heats of formation (kJ mol^{-1}) relevant to the $[CH_3CH_2CH_2OH]^{\cdot+}/[CH_2CH_2CH_2OH_2^+]$ system

Species	$\Delta_fH°_{298}$(exp)[a]	$\Delta_fH°_{298}$(calc)[b]
$CH_3CH_2CH_2OH^{\cdot+}$, **3a**	731 ± 2	713 ± 4
$^{\cdot}CH_2CH_2CH_2OH_2^+$, **3b**	714 ± 5 (701)[c]	688 ± 4
Transition structure, **3ab**	776	783 ± 4
$CH_3CHCH_2^+$	959	
H_2O	−242	
$CH_3CHCH_2^{\cdot+}$ + H_2O, **3c**	717	
c-$CH_2CH_2CH_2^{\cdot+}$	1004	
c-$CH_2CH_2CH_2^{\cdot+}$ + H_2O, **3d**	762	
$C_2H_5CHOH^+$	556	
$H^{\cdot}$	218	
$C_2H_5CHOH^+ + H^{\cdot}$, **3e**	774	
$C_2H_5^{\cdot}$	118	
CH_2OH^+	708	
$C_2H_5^{\cdot}$ + CH_2OH^+, **3f**	826	

[a] [17] unless otherwise specified.

[b] Estimated from the G2(MP2, SVP) atomization energies.

[c] Using the relationship [Eq. (7)]: $\Delta_fH°$[**3b**] = $\Delta_fH°(C_3H_7OH)$ + IE($H^{\cdot}$) + BDE(RCH_2-H) − PA(C_3H_7OH) with PA(C_3H_7OH) = 786 kJ mol^{-1} and $\Delta_fH°(C_3H_7OH)$ = −255 kJ mol^{-1} ([7]).

$[CH_2CH_2CH_2OH_2]^{\cdot+}$, **3b**, may be approximated by Eq. (7):

$$\Delta_f H^\circ[\mathbf{3b}] \approx \Delta_f H^\circ(C_3H_7OH) + IE(H^\cdot) + BDE(RCH_2\text{-}H) - PA(C_3H_7OH) \quad (7)$$

Surprisingly, the result, $\Delta_f H^\circ(\mathbf{3b}) = 701$ kJ mol^{-1}, is in poor agreement with the preceding experimental estimate.

Both metastable ions **3a** and **3b** eliminate a water molecule. Deuterium labeling unambiguously demonstrates that this elimination reaction involves specifically the hydroxyl group and one hydrogen of the methyl group of the propanol molecular ion [30,31]. Moreover, Wesdemiotis et al. [26] have shown that structures **3a** and **3b** are distinct species that may be characterized from their neutralization–reionization spectra. Thus the results seem to be understandable by the occurrence of a 1,4-hydrogen atom migration through a transition structure that is the highest point in the path connecting **3a** with the dehydration products. Accurate determination of the appearance energy for the $[C_3H_6]^{\cdot+}$ fragment ions from propanol has been made by photoelectron–photoion coincidence measurements [28]. This experimental value, added to $\Delta_f H^\circ$(propanol) = −255 kJ mol^{-1}, leads to an enthalpy level of 776 kJ mol^{-1} for the energy determining step of the dehydration process. Finally, the last experimental information to be considered is that, on the basis of differences observed in charge stripping mass spectra [30,31], ionized cyclopropane rather than ionized propene was suggested to be produced during the dehydration of ionized propanol, **3a**.

The first theoretical study on ionized propanol explored the reaction path **3a** → **3b** → [cyclo-$C_3H_6]^{\cdot+}$ + H_2O, at the 4-31G/STO-3G level [32]. A more elaborate study of the same reactions has been undertaken more recently at the MP2/6-31G** level by Booze and Baer [29a]. Clear discrepancies appear between theoretical and experimental energetic data. First of all, as underlined by Baer et al. [29], the photoelectron spectrum of propanol exhibits a broad and unresolved first band, suggesting an ion geometry significantly different from that of the neutral. This means that the ionization onset may correspond to a vibrationally excited ion, far above its ground state. The direct use of IE(propanol) = 10.22 eV may thus lead to an overestimation of the heat of formation of ionized propanol, an excess energy as large as 0.5 eV has been suggested [29]. The second point is that the experimental heat of formation of **3b** does not satisfactorily agree with estimates based on thermochemical scheme (701 kJ mol^{-1}, see above and Table 5) and, principally with molecular orbital calculations at the MP2/6-31G** level [29]. In fact, the experimentally derived $\Delta_f H^\circ(\mathbf{3b})$ value of 714 kJ mol^{-1} seems too high by 0.3 eV compared with the MP2/6-31G** calculations. This may be interpreted as an overestimation of the experimental $\Delta_f H^\circ(\mathbf{3b})$ value due to a nonnegligible kinetic shift effect during the appearance energy determination, as suggested by Baer et al. [29]. To summarize, a large part of the discrepancies observed between theory and experiment is removed by considering heat of formation values for **3a** (and **3b**) shifted by 50 (and 30) kJ mol^{-1} below the tabulated ones [29a]. It is therefore of interest to see if these conclusions remain unchanged when using the more elaborated G2(MP2, SVP) theory.

Our calculations indicate that the MP2/6-31G* structure of ionized propanol **3a** exhibits a long C(2)–C(3) bond (1.759 Å, Fig. 1) and a short C(2)–O(1) bond (1.342 Å, Fig. 1). This situation has also been observed at the MP2/6-31G** level [29a] and is comparable to that described previously for ionized ethanol **2a**. This C–C bond stretching is accompanied by the appearance of a significant spin density on carbon C(3) (Fig. 1). The most stable form of the distonic ion **3b** presents a "gauche" conformation. In this situation a stabilizing interaction is allowed between one of the O-bonded hydrogens (which bears a large positive charge) and the *p* orbital of the carbon atom C(4) (Fig. 1) where the lone electron is located (which constitutes a polarizable centre). The stabilisation brought by this internal hydrogen bond may be estimated by considering ion **3b** in its totally trans conformation. At the MP2/6-31G* level, this latter conformation is 11 kJ mol^{-1} above the most stable

Table 6
Calculated total (hartree) and relative (kJ mol^{-1}) energies involving the $[CH_3CH_2CH_2OH]^{\cdot+}/[CH_2CH_2CH_2OH_2^{+}]$ system

Level of theory	E(**3a**)	ΔE(**3b**)[a]	ΔE(**3ab**)[a]	ΔE(**3c**)[a] ($CH_3CHCH_2^{\cdot+}$ + H_2O)	ΔE(**3d**)[a] (c-$CH_2CH_2CH_2^{+}$ + H_2O)	ΔE(**3e**)[a] ($C_2H_5CHOH^{+}$ + $H^{\cdot}$)	ΔE(**3f**)[a] ($C_2H_5^{\cdot}$ + CH_2OH^{+})
HF/6-31G*	−192.77451	−50	81				
ZPE(HF/6-31G*)	265	268	260	249	251	245	251
MP2(FC)/6-31G*	−193.33031	−13	105	37	80	24	117
QCISD(T)/6-31G*	−193.39365	−11	71	32	77	34	109
MP2/6-311+G(3df,2p)	−193.58556	−20	110	13	54	44	119
G2(MP2, SVP)	−193.61202	−18 (−25)	76 (71)	8 (9)	50 (52)	55 (56)	110 (113)

[a] Relative energies including ZPE corrections, and, in parentheses, 298 K enthalpy corrections.

folded structure presented in Fig. 1. The transition structure **3ab** adopts a half-chair conformation with O . . . H and C . . . H distances (1.693 Å and 1.165 Å, respectively) close to those encountered in the reactant nearest in energy, i.e. **3a**.

Considering the doubt raised on the validity of the tabulated $\Delta_f H°$(**3a**) and $\Delta_f H°$(**3b**) values, it seems appropriate to anchor the computational results to more secure data. For this purpose, we considered four sets of species for which the heats of formation are unambiguously known and that are also possible dissociation products of **3a** and **3b**. Two of them are the dehydration products: $[propene]^{\cdot+}$ + H_2O, **3c**, and $[cyclopropane]^{\cdot+}$ + H_2O, **3d**; the two others may originate from **3a** by simple bond fissions: $[C_2H_5CHOH]^{+}$ + $H^{\cdot}$, **3e** and $[CH_2OH]^{+}$ + $C_2H_5^{\cdot}$, **3f**. Experimental and theoretical data for these four sets of products as well as **3a** and **3b** are reported in Tables 5 and 6.

When comparing the data of Table 5 and Table 6, it appears clear that, indeed, the tabulated heats of formation of **3a** and **3b** should be lowered in order to reconcile theory and experiment. This may be seen immediately by looking at the experimental and theoretical estimates of $\Delta_f H°$(**3a**) and $\Delta_f H°$(**3b**) quoted in Table 5. Both values calculated from atomization and dissociation energies are lower than the tabulated $\Delta_f H°$(exp). The shift predicted by G2(MP2, SVP) calculations with respect to the tabulated values is 18 kJ mol^{-1} for **3a** and 26 kJ mol^{-1} for **3b**. This confirms the conclusion drawn by Baer et al. [29] that the tabulated heat of formation of both species was overestimated. The G2(MP2, SVP) results suggest, however, a less dramatic shift than originally proposed, particularly for **3a**.

Another surprising result is the difference observed between the calculated $\Delta_f H°$(**3b**) (688 kJ mol^{-1}) and the estimate based on a thermochemical cycle [701 kJ mol^{-1} from Eq. (7)]. In fact, the reason for the discrepancy is straightforward. When using the thermochemical cycle it is assumed that the energy change is exclusively due to the O-protonation and the C–H bond dissociation processes. No other stabilizing effect is considered. This assumption is not valid here because **3b**, in its most stable conformation, contains an internal hydrogen bond. The estimate given by the calculation for the corresponding energy gain, 11 kJ mol^{-1} (MP2/6-31G* level), is in good agreement with the above mentioned $\Delta_f H°$ shift (13 kJ mol^{-1}).

Finally, an important result concerns the calculated critical energy for the 1,4-hydrogen migration (reaction III). This reaction is predicted to have an activation barrier of 70 kJ mol^{-1}. By using the G2(MP2, SVP) heat of formation value obtained above, $\Delta_f H°$(**3a**) = 713 kJ mol^{-1} (Table 5), we predict for the transition structure $\Delta_f H°$(**3ab**) = 783 kJ mol^{-1} in correct agreement with the experimental threshold measured for the dehydration of ionized propanol (776 kJ mol^{-1}) [28]. Thus, it strongly suggests that the energy determining step of the dehydration of ionized propanol is effectively the 1,4-hydrogen migration **3a** → **3b**. This is also in keeping with the earlier proposal, based on MO calculation [29], that the formation of the products $[cyclopropane]^{\cdot+}$ + H_2O, **3d** from **3b** is an anchimerically assisted process

Table 7
Experimental and calculated heats of formation (kJ mol^{-1}) relevant to the $[CH_3CH_2CH_2CH_2OH]^{\cdot+}/[CH_2CH_2CH_2CH_2OH_2^+]$ system

Species	$\Delta_f H^\circ_{298}$(exp)[a]	$\Delta_f H^\circ_{298}$(calc)[b]
$CH_3CH_2CH_2CH_2OH^{\cdot+}$, **4a**	689 ± 2	677 ± 7
$^{\cdot}CH_2CH_2CH_2CH_2OH_2^+$, **4b**	(678)[c]	643 ± 7
Transition structure, **4ab**	707	696 ± 7
E-$CH_3CHCHCH_3^+$	866	
H_2O	−242	
$CH_3CHCHCH_3^+ + H_2O$, **4c**	624	
$CH_3CH_2CHCH_2^+$	924	
H_2O	−242	
$CH_3CH_2CHCH_2^+ + H_2O$, **4d**	682	
$H^{\cdot}$	218	
$C_3H_7CHOH^+$	530	
$C_3H_7CHOH^+ + H^{\cdot}$, **4e**	748	
n-$C_3H_7^{\cdot}$	100	
CH_2OH^+	708	
n-$C_3H_7^{\cdot} + CH_2OH^+$, **4f**	808	

[a] [17] unless otherwise specified.
[b] Estimated from the G2(MP2, SVP) atomization energies.
[c] Using the relationship: $\Delta_f H^\circ[\mathbf{4b}] = \Delta_f H^\circ(C_4H_9OH) + IE(H^{\cdot}) + BDE(RCH_2\text{-}H) - PA(C_4H_9OH)$ with $PA(C_4H_9OH) = 789$ kJ mol^{-1} and $\Delta_f H^\circ(C_4H_9OH) = -275$ kJ mol^{-1}.

that needs no extra energy other than the corresponding reaction endothermicity.

3.4. $[C_4H_9OH]^{\cdot+}/[C_4H_8OH_2]^{\cdot+}$

The experimental thermochemistry of this system is summarized in Table 7. The heat of formation of ionized butanol (689 kJ mol^{-1}) is obtained by combining its adiabatic ionization energy, IE(butanol) = 9.99 eV [33], and heat of formation $\Delta_f H^\circ$(butanol) = −275 kJ mol^{-1} [17]. No experimentally determined heat of formation is available for the distonic ion **4b**. The procedure based on a thermochemical cycle comparable to that described in Scheme 2 may be used, however. This procedure allows derivation of an estimate of $\Delta_f H^\circ(\mathbf{4b}) = 678$ kJ mol^{-1} from Eq. (8):

$$\Delta_f H^\circ(\mathbf{4b}) \approx \Delta_f H^\circ(C_4H_9OH) + IE(H^{\cdot}) + BDE(RCH_2\text{-}H) - PA(C_4H_9OH) \quad (8)$$

In contrast to the preceding systems, both structures **4a** and **4b** present very similar collisional activation and neutralization–reionization spectra, pointing to a facile isomerization [26]. Moreover, Wesdemiotis et al. [26] concluded from their experiments that the equilibrium between **4a** and **4b** is strongly displaced toward the latter structure, pointing to its greater stability. The exclusive dissociation of metastable ions **4a** is the water loss and this fragmentation is accompanied by the release of a small translational energy ($T_{0.5}$ = 2 meV [34b]. Deuterium labeling shows that the water molecule expelled preferentially contains the hydroxylic hydrogen and one from the methyl group, but significant hydrogen/deuterium (H/D) scrambling precedes the fragmentation both at high [34a] or low [34b] internal energy.

The thermochemistry and dissociation rate of energy-selected butanol ions, **4a**, have been determined by photoionization [33]. The onset for the loss of H_2O lies 982 ± 5 kJ mol^{-1} above neutral butanol, i.e. at a 300 K enthalpy level of 707 ± 5 kJ mol^{-1}. The slow rate observed for this reaction is only compatible with a dehydration process occurring via a stable intermediate structure such as **4b**. Moreover, the dissociation of the parent ions has been analyzed by a two components decay that was attributed to the formation of (at least) two product ions, in which the most stable of the various $[C_4H_8]^{\cdot+}$ isomers, i.e. [2-butene]$^{\cdot+}$, has been considered.

The MP2/6-31G* geometry of **4a** reported in Fig. 1 again reveals a large C(2)–C(3) bond (1.746 Å) associated with a short C(2)–O(1) bond (1.344 Å). This is comparable with the results obtained for the two other ionized alkanol structures (**2a** and **3a**) and, similarly, a large part of the spin density is borne by the carbon atom C(3) (Fig. 1). The most stable conformation of the distonic ion **4b** is a pseudo-chair conformation that leads to the 1,5-H migration process. The stability of this conformation is, essentially, due to the favourable electrostatic interaction between a positively charged hydrogen atom [H(15), Fig. 1] and the polarizable radical centre on C(5). An indication of the energy gain brought by this internal hydrogen bond is provided by the calculation of energy of the completely trans conformation of **4b**. At

Table 8
Calculated total (hartree) and relative (kJ mol^{-1}) energies involving the $[CH_3CH_2CH_2CH_2OH]^{\cdot+}$/$[CH_2CH_2CH_2CH_2OH_2^{\cdot+}]$ system

Level of theory	E(**4a**)	ΔE(**4b**)[a]	ΔE(**4ab**)[a]	ΔE(**4c**)[a] ($CH_3CHCHCH_3^+$ + H_2O)	ΔE(**4d**)[a] ($CH_3CH_2CHCH_2^+$ + H_2O)	ΔE(**4e**)[a] ($C_3H_7CHOH^+$ + H$^{\cdot}$)	ΔE(**4f**)[a] (n-$C_3H_7^{\cdot}$ + CH_2OH^+)
HF/6-31G*	−231.81082	−67	33				
ZPE(HF/6-31G*)	342	337	332	320	321	317	324
MP2(FC)/6-31G*	−232.49955	−35	21	−24	34	25	127
QCISD(T)/6-31G*	−232.57905	−33	25	−30	27	35	118
MP2/6-311+G(3df,2p)	−232.80829	−44	15	−48	9	46	129
G2(MP2, SVP)	−232.83767	−42 (−34)	19 (19)	−55 (−45)	2 (11)	55 (63)	119 (128)

[a] Relative energies including ZPE corrections and, in parentheses, 298 K enthalpy corrections.

the MP2/6-31G* level, this structure is calculated to lie 37 kJ mol^{-1} above the most stable, folded, conformation of this ion (Fig. 1).

Finally, the transition structure for 1,5-hydrogen migration, **4ab**, enjoys a pseudo-half chair conformation with O(1)–H(15) and H(15)–C(5) distances equal to 1.662 and 1.178 Å, respectively. Thus, it appears that the C–H bond is far from being broken and the O–H bond is far from being formed in this transition structure that is closest in structure and in energy to the reactant **4a**.

The energetics of this system have been explored by considering not only the two isomers **4a** and **4b**, but also four sets of products: $[CH_3CHCHCH_3]^{\cdot+}$ + H_2O, **4c**; $[CH_3CH_2CHCH_2]^{\cdot+}$ + H_2O, **4d**: $[C_3H_7CHOH]^+$ + H$^{\cdot}$, **4e**; and $[CH_2OH]^+$ + n-$C_3H_7^{\cdot}$, **4f**. The first corresponds to the most stable dehydration products and the last two to possible dissociation products of **4a** via simple cleavage processes.

The G2(MP2, SVP) calculations summarized in Tables 7 and 8 indicate an enthalpy difference of −34 kJ mol^{-1} between **4a** and **4b**, a value that compares poorly with the estimate based on $\Delta_f H^\circ_{298}$ derived from experimental data and Eq. (8) (11 kJ mol^{-1}). This point may be clarified by examining separately each individual case. The mean value of $\Delta_f H^\circ$(**4a**) deduced from atomization and dissociation energies of **4a** is equal to 677 kJ mol^{-1} with a standard deviation as large as ±7 kJ mol^{-1}. Because of computational and experimental uncertainties this value is in marginal agreement with the experimental value of 689 kJ mol^{-1}. This means that the tabulated heat of formation of **4a** may support a lowering by ∼10 kJ mol^{-1}.

The heat of formation of **4b** estimated by use of the G2(MP2, SVP) atomization or dissociation energies is equal to 643 kJ mol^{-1}. This is clearly less than the estimate of 678 kJ mol^{-1} based on a simplified thermochemical cycle [Eq. (8)]. As established for **3d** this discrepancy is due to the neglect of the internal hydrogen bond between the oxygen bonded H atom and the radical centre. As indicated above in the case of **4b**, this favourable electrostatic interaction provides an extra stabilization of ∼37 kJ mol^{-1}. This effect is not allowed for in the $\Delta_f H^\circ$(**4b**) estimated from Eq. (8), and, accordingly, the two $\Delta_f H^\circ$(**4b**) values quoted in Table 7 differ by 35 kJ mol^{-1}.

The calculated barrier height for the 1,5-hydrogen migration is situated 19 kJ mol^{-1} above **4a**. On an enthalpy scale it corresponds to $\Delta_f H^\circ$(**4ab**) = 696 kJ mol^{-1}. Considering the computational and experimental uncertainties, this value is comparable to the experimental threshold for the dehydration of ionized butanol (707 ± 5 kJ mol^{-1}) [33]. It is thus highly probable that the energy determining step for the dehydration reaction is the initial 1,5-H migration. After this first step, the distonic ion **4b** contains an excess energy of 54 kJ mol^{-1} that it may use to undergo the subsequent reaction steps leading to water loss.

Finally, a brief comparison of the present data with the relevant neutral system may be made. The Barton type rearrangement [5] involves a 1,5 hydrogen atom migration from a carbon to a radical site located on an

oxygen atom. It is thus the exact neutral equivalent of reaction IV. The activation energy experimentally determined [1] and theoretically confirmed [4] for the Barton reaction is ~40 kJ mol^{-1}. The critical energy value calculated in the present study for reaction IV (19 kJ mol^{-1}) clearly demonstrates a significant lowering of the energy barrier when the reactive species is a radical cation. This may be considered another illustration of the so-called "hole catalysis" concept [35]. The lowering of the activation barrier may be qualitatively understood by examining the calculated electron distribution. After removal of one electron from butanol, an important charge redistribution occurs in the molecular ion with the net result that all hydrogen atoms are positively charged (from 0.23 to 0.56, as indicated by a Mulliken analysis of **4a**). As long as the oxygen atom is negatively charged (−0.49 in **4a**), the approach of a hydrogen atom of the methyl group to the oxygen is highly favoured ("catalyzed") by this electrostatic interaction.

3.5. Ring strain energy and barrier height

As expected, the barrier for hydrogen shift decreases in the order 1,2 > 1,3 > 1,4 > 1,5-H. This is clearly illustrated by the schematic energy profiles shown in Fig. 2.

A first observation is that the barrier heights for 1,2- and 1,3-hydrogen shifts are very similar; they fall in a limited energy range situated near 90–100 kJ mol^{-1} with respect to the corresponding ionized alcohols. This is consistent with the high, comparable ring strain energies for three and four membered ring structures. Accordingly, structures **1ab** and **2ab** are cyclic species characterized by HCO or HCC angles of 52.5° and 89.1°, respectively. By comparison, the ring strain energies of cyclopropane and cyclobutane are equal to 115 and 110 kJ mol^{-1}, respectively [36].

For 1,4- and 1,5-hydrogen migration no such spectacular ring strain effect is expected (the ring strain energies of cyclopentane and cyclohexane are 26 and 1 kJ mol^{-1}, respectively). There is, however, a large difference between the two critical energies: the barrier for 1,4-hydrogen shift is close to that of the

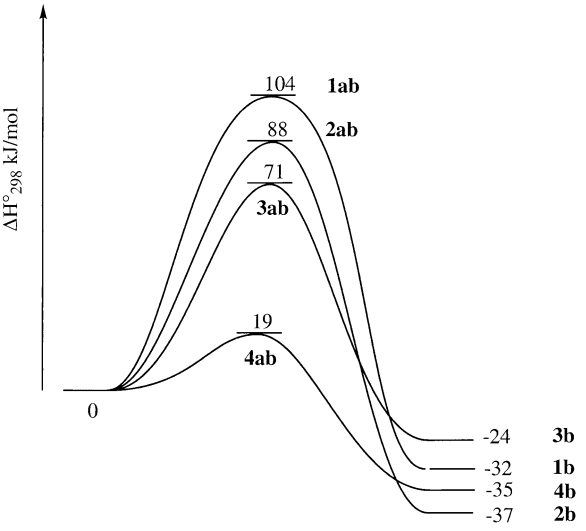

Fig. 2. Calculated 298 K enthalpy change for intramolecular hydrogen migrations in ionized alcohols.

1,3-hydrogen shift and almost four times higher than that for the 1,5-hydrogen migration. A probable reason for this considerable difference is that a large unfavourable electrostatic interaction destabilizes the transition structure for 1,4-hydrogen shift, i.e. **3ab**. Accordingly, when considering the charge distribution in **3ab** and in **4ab** it appears that most of the positive charge is shared between the methylene group bearing the hydroxyl function and the terminal methyl group. It is evident that the distance between these two positively charged centres is lower in the cyclic structure **3ab** than in **4ab** [the C(2) . . . C(4) and C(2) . . . C(5)] distances are 2.38 Å and 3.13 Å in **3ab** and **4ab**, respectively). Consequently, the structure **3ab** is more efficiently destabilized than **4ab**. Note that neither **1ab** nor **2ab** may suffer this phenomenon because the two carbon atoms involved are either identical or participate in the same bond.

4. Conclusion

The present G2(MP2, SVP) molecular orbital calculations confirm the greater stability of the distonic ions $[H(CH_2)_{n-1}OH]^{\cdot+}$ with respect to their conventional isomers $[H(CH_2)_{n-1}OH]^{\cdot+}$. In addition, we

note that the estimates of the heat of formation of distonic ions via "simple" thermochemical cycles may lead to significant overestimates due to the neglect of internal stabilization by hydrogen bonding.

The barrier height for the 1,*n*-hydrogen migration $[H(CH_2)_{n-1}OH]^{\cdot+} \rightarrow [(CH_2)_{n-1}OH_2]^{\cdot+}$ decreases when the number of carbon atoms, *n*, increases. It appears that both 1,2- and 1,3-hydrogen migrations, I and II, have comparable critical energies, close to 100 kJ mol^{-1}. For 1,4- and 1,5-hydrogen migrations, the computed critical energies are reduced to 70 kJ mol^{-1} and 19 kJ mol^{-1} for reactions III and IV, respectively. A comparison between the critical energies associated with the 1,5-hydrogen migration in ionized butanol (19 kJ mol^{-1}) and the corresponding neutral free radical (40 kJ mol^{-1}) reveals a clear barrier lowering that may be interpreted by a catalytic effect of the positive charge during the hydrogen atom migration.

References

[1] (a) M. Lazar, J. Rychly, V. Klimo, P. Pelikan, L. Valko, Free Radicals in Chemistry and Biology, CRC, Boca Raton, 1989; (b) M. Regitz, B. Giese, Methoden der organishen Chemie (Houben Weyl), Vol. E19, Georg Theime, Stuttgart, 1989.

[2] (a) G. Bouchoux, Mass Spectrom. Rev. 7 (1988) 1; G. Bouchoux, Mass Spectrom. Rev. 7 (1988) 203; (b) S. Hammerum, Mass Spectrom. Rev. 7 (1988) 123; (c) J. S. Splitter, in Applications of Mass Spectrometry to Organic Stereochemistry, J. S. Splitter, F. Turecek (Eds.), VCH, New York, 1994, p. 39; (d) R. L. Smith, P. K. Chou, H. I. Kenttämaa, in The Structure, Energetics and Dynamics of Organic Ions, T. Baer, C. Y. Ng, I. Powis (Eds.), Wiley, Chichester, 1996, p. 199.

[3] B. Viskolcz, G. Lendvay, T. Körtvelyesi, L. Seres, J. Am. Chem. Soc. 118 (1996) 3006.

[4] G. Hornung, C. A. Schalley, M. Dieterle, D. Schröder, H. Schwarz, Chem. Eur. J. 3 (1997) 1866.

[5] D. H. R. Barton, J. M. Beaton, L. E. Geller, M. M. Pechet, J. Am. Chem. Soc. 83 (1961) 4076.

[6] B. F. Yates, L. Radom, J. Am. Chem. Soc. 109 (1987) 2910.

[7] R. Lin, P. Pulay, J. Comp. Chem. 13 (1992) 183; (b) A. E. Dorigo, M. A. Mc Carrick, R. J. Loncharich, K. N. Houk, J. Am. Chem. Soc. 112 (1990) 7508; (c) G. Bouchoux, A. Luna, J. Tortajada, Int. J. Mass Spectrom. Ion Processes 167/168 (1997) 353; (d) W. Bertrand, G. Bouchoux, Rapid Commun. Mass Spectrom. 12 (1998) 1697.

[8] (a) W. J. Bouma, R. H. Nobes, L. Radom, J. Am. Chem. Soc. 104 (1982) 2929; (b) J. W. Gauld, H. E. Audier, J. Fossey, L. Radom, J. Am. Chem. Soc. 118 (1996) 6299; (c) J. W. Gauld, L. Radom, J. Am. Chem. Soc. 119 (1997) 9831; (d) J. Fossey, P. Mourgues, H. E. Audier, unpublished; (e) J. W. Gauld, M. N. Glukhovtsev, L. Radom, Chem. Phys. Lett. 262 (1996) 187; (f) J. W. Gauld, J. L. Holmes, L. Radom, Acta Chem. Scand. 51 (1997) 641.

[9] (a) G. Bouchoux, N. Choret, R. Flammang, unpublished; (b) See also [30, 31, 33].

[10] F. Turecek, in The Chemistry of Hydroxyl, Ether and Peroxide Groups, Suppl. E2, S. Pataï (Ed.), Wiley, Chichester, 1993, p. 373.

[11] M. J. Frisch, G. W. Trucks, H. B. Schlegel, P. M. W. Gill, B. G. Johnson, M. A. Robb, J. R. Cheesemann, T. A. Keith, G. A. Petersson, J. A. Montgomery, K. Raghavachari, M. A. Al-Laham, V. G. Zakrewski, J. V. Ortiz, J. B. Foresman, J. Cioslowski, B. B. Stefanov, A. Nanayakkara, M. Challacombe, C. Y. Peng, P. Y. Ayala, W. Chen, M. W. Wong, J. L. Andres, E. S. Replogle, R. Gomperts, R. L. Martin, D. J. Fox, J. S. Binkley, D. J. Defrees, J. Baker, J. P. Stewart, M. Head-Gordon, C. Gonzales, J. A. Pople, GAUSSIAN 94, Revision, Gaussian Inc., Pittsburgh, PA, 1995.

[12] (a) A. P. Scott, L. Radom, J. Phys. Chem. 100 (1996) 16 502; (b) J. A. Pople, A. P. Scott, M. W. Wong, L. Radom, Isr. J. Chem. 33 (1993) 345.

[13] P. M. Mayer, C. J. Parkinson, D. M. Smith, L. Radom, J. Chem. Phys. 108 (1998) 604.

[14] L. A. Curtiss, K. Raghavachari, G. W. Trucks, J. A. Pople, J. Chem. Phys. 94 (1991) 7221.

[15] L. A. Curtiss, K. Raghavachari, J. A. Pople, J. Chem. Phys. 98 (1993) 1293.

[16] (a) L. A. Curtiss, P. C. Redfern, B. J. Smith, L. Radom, J. Chem. Phys. 104 (1996) 5148; (b) B. J. Smith, L. Radom, J. Phys. Chem. 99 (1995) 6468; (c) A. Nicolaides, A. Rauk, M. N. Glukhovtsev, L. Radom, J. Phys. Chem. 100 (1996) 17 460.

[17] (a) S. G. Lias, J. E. Bartmess, J. F. Liebman, J. L. Holmes, R. D. Levin, W. G. Mallard, J. Phys. Chem. Ref. Data 1 (1988) 17 (suppl); (b) E. P. L. Hunter, S. G. Lias, J. Phys. Chem. Ref. Data 27 (1998) 413 (and http://webbook.nist.gov).

[18] (a) J. Berkowitz, J. Chem. Phys. 69 (1978) 3044; (b) J. Momigny, H. Wankenne, C. Krier, Int. J. Mass Spectrom. Ion Phys. 35 (1980) 151; (c) J. L. Holmes, F. P. Lossing, J. K. Terlouw, P. C. Burgers, J. Am. Chem. Soc. 104 (1982) 2931; (d) W. J. Bouma, J. K. MacLeod, L. Radom, J. Am. Chem. Soc. 104 (1982) 2930.

[19] K. M. A. Refaey, W. A. Chupka, J. Chem. Phys. 48 (1968) 5205.

[20] J. W. Gauld, L. Radom, J. Phys. Chem. 98 (1994) 777.

[21] P. M. Mayer, M. N. Glukhovtsev, J. W. Gauld, L. Radom, J. Am. Chem. Soc. 119 (1997) 12 889.

[22] H. E. Audier, J. Fossey, P. Mourgues, D. Leblanc, S. Hammerum, Int. J. Mass Spectrom. Ion Processes 157/158 (1996) 275.

[23] (a) B. Ruscic, J. Berkowitz, J. Phys. Chem. 97 (1993) 11 451; (b) R. Dóbé, T. Bérces, F. Márta, J. Grussdorf, F. Temps, H. G. Wagner, J. Phys. Chem. 100 (1996) 19 864.

[24] J. K. Terlouw, W. Heerma, G. Dijkstra, Org. Mass Spectrom. 16 (1981) 326.

[25] V. H. Wysocki, H. I. Kenttämaa, J. Am. Chem. Soc. 112 (1990) 5110.
[26] C. Wesdemiotis, P. O. Danis, R. Feng, J. Tso, F. W. McLafferty, J. Am. Chem. Soc. 107 (1985) 8059.
[27] (a) W. J. Bouma, R. H. Nobes, L. Radom, J. Am. Chem. Soc. 105 (1983) 1743; (b) J. W. Gauld, L. Radom, Chem. Phys. Lett. 275 (1997) 28.
[28] J. D. Shao, T. Baer, J. C. Morrow, M. L. Fraser-Monteiro, J. Chem. Phys. 87 (1987) 5242.
[29] (a) J. A. Booze, T. Baer, J. Phys. Chem. 96 (1992) 5710; (b) J. A. Booze, T. Baer, J. Phys. Chem. 96 (1992) 5715.
[30] J. L. Holmes, A. A. Mommers, J. E. Szulejko, J. K. Terlouw, J. Chem. Soc. Chem. Commun. (1984) 165.
[31] R. D. Bowen, A. W. Colburn, P. J. Derrick, J. Am. Chem. Soc. 113 (1991) 1132.
[32] T. Takeuchi, S. Ueno, M. Yamamoto, T. Matsushita, K. Nishimoto, Int. J. Mass Spectrom. Ion Processes 64 (1985) 33.
[33] J. D. Shao, T. Baer, D. K. Lewis, J. Phys. Chem. 92 (1988) 5123.
[34] (a) G. J. Bukovits, H. Budzikiewicz, Org. Mass Spectrom. 18 (1983) 219; (b) D. J. McAdoo, C. E. Hudson, Org. Mass Spectrom. 22 (1987) 615.
[35] N. L. Bauld, J. Am. Chem. Soc. 114 (1992) 5800, and references therein.
[36] S. W. Benson, Thermochemical Kinetics, 2nd edn., Wiley, New York, 1976.